Unimolecular Reaction Dynamics from Kinetic Energy Release Distributions. 8. Protonated Fluorobenzene and Structure of the Phenyl Ion

J. C. Lorquet* and A. J. Lorquet

Département de Chimie, Université de Liège, Sart-Tilman (B6), B-4000 Liège 1, Belgium

Received: November 9, 2000; In Final Form: January 16, 2001

A previous interpretation of the kinetic energy release distribution (KERD) observed in the fragmentation of protonated fluorobenzene is confirmed by a maximum entropy analysis. The KERD is bimodal, with an intense and broad component due to the production of the cyclic phenyl ion. Ab initio calculations indicate the existence of several open-chain isomers, with an energy about 1.0−1.2 eV higher than that of the phenyl ring. A weaker component of the KERD corresponds to the formation of one or several of these acyclic structures. Its abundance represents about 6% of the main component (but drops down to 3% for the perdeuterated isomer). More translational energy than the statistical estimate is released during the dissociation process because of the presence of a barrier along the reaction path leading to the generation of the cyclic phenyl ion. About one-half of the energy of the barrier is released as translation, thereby indicating the operation of strong exit−channel interactions between separating fragments.

1. Introduction

Kinetic energy release distributions (KERDs) have long been considered to provide an essential piece of information in the study of reaction mechanisms of gaseous molecular ions.[1−13] The information is presented as a function, denoted $P(\epsilon|E)$, giving the probability of generating fragments with a relative translational energy equal to ϵ, if E denotes the internal energy measured in excess of the dissociation threshold.

Recently, Schröder and co-workers[14] published an analysis of the KERD derived from the decomposition on the microsecond time scale of the protonated fluorobenzene ion $C_6H_5F{\cdot}H^+ \rightarrow C_6H_5^+ + HF$. They showed that the dissociation process was composite. The most intense component of the KERD, characterized by a large translational energy release, was assigned to the production of the low-energy phenyl ion in its cyclic structure. This component of the KERD reaches its maximum at a value of (435 ± 40) meV for $C_6H_5F{\cdot}H^+$ and at about (550 ± 50) meV for the perdeuterated species $C_6D_5F{\cdot}D^+$. This reaction channel will henceforth be referred to as the "broad component". In addition, a weaker component (referred to as "medium" by Schröder et al.) is also observed. The corresponding most probable translational energy release is about (30 ± 10) meV for the normal compound and (40 ± 10) meV for the deuterated isotopomer, thus indicating a much smaller and much sharper translational energy release than that of the broad component. The intensity of the second component is much weaker than that of the main reaction channel, especially for the deuterated compound. The reactive fluxes are estimated to be roughly in the ratio 10:1 for $C_6H_5F{\cdot}H^+$ and 18:1 for $C_6D_5F{\cdot}D^+$. Having discarded possible alternative interpretations, Schröder et al. assigned this second channel to production of an open-chain phenyl ion. Typical plots of the KERDs are given in Figures 1 and 2.

A cross-section of the potential energy surface has been calculated ab initio by the same team for the production of the low-energy $C_6H_5^+$ cyclic isomer.[15] Barriers are found along the reaction path, giving rise to two nonplanar transition states. As a result, a substantial fraction of this (fairly large) barrier energy is expected to be released as translational energy. These barriers are followed by a potential well (0.42 eV deep) whose minimum corresponds to an ion-neutral complex $C_6H_5^+{\cdot}HF$. Vibrational frequencies of all stationary points have been computed for both isotopomers. Using the Rice−Ramsperger−Kassel−Marcus theory, Schröder et al.[14] estimated the internal energy E necessary to generate a protonated fluorobenzene ion with a lifetime in the metastable range (i.e., corresponding to lifetimes of the order of 10^{-5} s). A larger amount of energy must obviously be delivered to the deuterated compound to reach the same lifetime as the nondeuterated isotopomer.

This article attempts to analyze the experimental results obtained by Schröder and co-workers[14] on the basis of a model potential energy surface, represented in Figure 3. For simplicity, the two nonplanar transition states have been reduced to a single one, assumed to be located at an energy $E_b = 1.17$ eV above the dissociation asymptote.

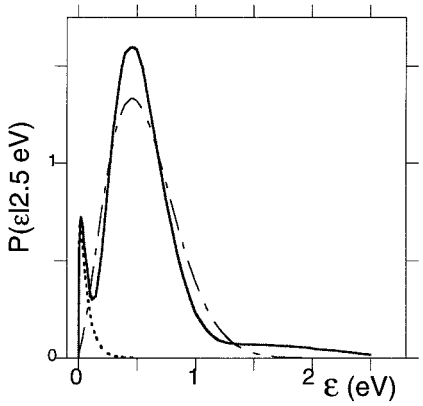

Figure 1. (solid line) Experimental KERD (obtained as private communication from the authors of ref 14) for the reaction $C_6H_5F{\cdot}H^+ \rightarrow C_6H_5^+ + HF$. (broken lines) Maximum entropy decomposition into two components assuming an internal energy of 2.50 eV. (dashed−dotted line) Generation of the cyclic phenyl ion. (dotted line) Production of a low-energy, open-chain isomer.

* E-mail: jc.lorquet@ulg.ac.be.

10.1021/jp004143j CCC: $20.00
Published on Web 03/27/2001

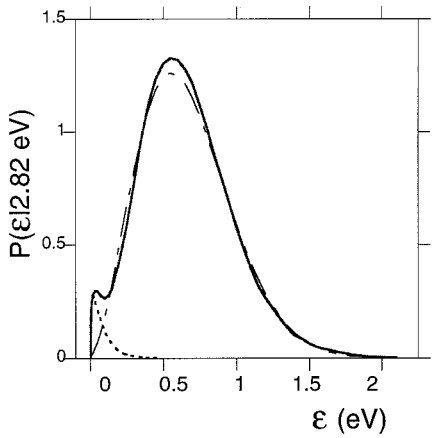

Figure 2. (solid line) Experimental KERD determined in ref 14 for the reaction $C_6D_5F{\cdot}D^+ \rightarrow C_6D_5^+ + DF$. (broken lines) Maximum entropy decomposition into two components assuming an internal energy of 2.82 eV. (dashed−dotted line) Generation of the cyclic phenyl ion. (dotted line) Production of a low-energy, open-chain isomer.

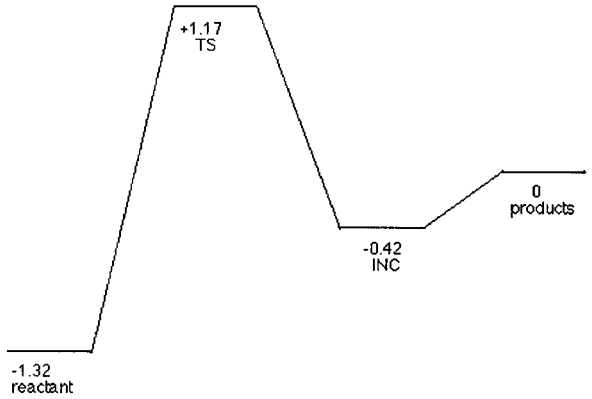

Figure 3. Schematic potential energy diagram for the fragmentation of protonated fluorobenzene. Relative energies in eV. TS, transition state; INC, ion−neutral complex.

Based on the estimates of Schröder et al.,[14] we consider the fate of a $C_6H_5F{\cdot}H^+$ ion having an internal energy of 2.50 eV above the dissociation asymptote and compare it with that of a $C_6D_5F{\cdot}D^+$ ion with 2.82 eV internal energy.

The approach adopted in this article is as follows. The maximum entropy method is summarized and applied, in the form of a surprisal analysis, to the study of the KERDs measured by Schröder and co-workers.[14] The average kinetic energy release is partitioned into two components of the energy in excess [i.e., the energy of the barrier E_b, and the nonfixed energy of the transition state $(E - E_b)$]. Both components are partly converted into translational energy, but with different efficiencies. The energy of the barrier is preferentially released as translational energy, with a higher efficiency than the internal energy in excess of the barrier $(E - E_b)$. The weaker component of the KERD is assigned to the production of a $C_6H_5^+$ open-chain isomer whose possible low-energy structures are studied by ab initio calculations. The experimentally determined bimodal KERD is then interpreted as the sum of two contributions, as originally suggested by Schröder and co-workers.

2. The Maximum Entropy Method

The method has been described several times, both in general terms[16−20] and in the context of mass-spectrometric experimentation.[4,5,11,21−28] It consists of comparing the actual, experimentally determined KERD, denoted $P(\epsilon|E)$, with a hypothetical distribution, denoted the prior distribution $P^o(\epsilon|E)$, which would be observed if the dissociation proceeded in a completely statistical way, that is, if all available quantum states of the pair of fragments were populated with the same probability. Both KERDs are assumed to be normalized, that is,

$$\int_0^E P(\epsilon|E)\mathrm{d}\epsilon = \int_0^E P^0(\epsilon|E)\mathrm{d}\epsilon = 1 \qquad (1)$$

According to the maximum entropy theory, these two KERDs are related by the following equation:

$$P(\epsilon|E) = P^0(\epsilon|E)\, \mathrm{e}^{-\lambda_0}\, \mathrm{e}^{-\lambda_1 A_1}\, \mathrm{e}^{-\lambda_2 A_2} \ldots \qquad (2)$$

where A_1 and A_2 denote (up to this point unknown) physical properties that prevent the energy partitioning from being fully statistical. They are therefore referred to as "informative observables" or "dynamical constraints". The quantities λ_0, λ_1, and λ_2 are Lagrange multipliers in a process that consists of maximizing the entropy, that is, in making the dissociation dynamics as statistical as allowed by the constraint(s). In practice, however, the quality of the experimental data is such that only a single constraint can be identified, so that eq 2 reduces to

$$P(\epsilon|E) = P^0(\epsilon|E)\, \mathrm{e}^{-\lambda_0}\, \mathrm{e}^{-\lambda_1 A} \qquad (3)$$

This is a one-parameter equation, because the Lagrange multiplier λ_0 can be determined by the normalization condition (eq 1).

A convenient way to identify the nature of the constraint consists of conducting a so-called "surprisal analysis".[4,5,16−21,25] From eq 3, one derives

$$I \equiv \ln\left[\frac{P^0(\epsilon|E)}{P(\epsilon|E)}\right] = \lambda_0 + \lambda_1 A \qquad (4)$$

The quantity I, denoting the surprisal, is then plotted as a function of various variables. The variable that generates a linear plot is identified as the constraint A.

To perform this analysis, the prior distribution has to be calculated. In a dissociation process, the internal energy E partitions into a translational component ϵ, whereas the remainder $(E - \epsilon)$ is stored in the vibrational−rotational degrees of freedom of the pair of fragments. Because the density of translational states in a three-dimensional space is proportional to $\epsilon^{1/2}$, the prior distribution is simply given by[1,16−20,23−29]

$$P^0(\epsilon|E) = A(E)\epsilon^{1/2}N(E - \epsilon) \qquad (5)$$

where $N(E - \epsilon)$ denotes the density of vibrational−rotational states of the pair of fragments. $A(E)$ is a normalization coefficient that can be obtained by substituting eq 5 into eq 1.

The functions $N(E)$ representing the density of states of the pair of fragments $C_6H_5^+ + HF$ and that relative to $C_6D_5^+ + DF$ have been calculated by the direct-count method[1,30] assuming a cyclic structure for the phenyl ion. The necessary rotational constants and vibrational frequencies have been calculated ab initio at the B3LYP/6-31G(d) level recommended by Scott and Radom[31] and scaled according to their prescriptions. The agreement with the set of vibrational frequencies previously calculated by Klippenstein[32] for the $C_6H_5^+$ ion is excellent. It turns out that the density of states can be nicely fitted to an analytical expression

$$N(E) = C \exp(\beta\sqrt{E}) \qquad (6)$$

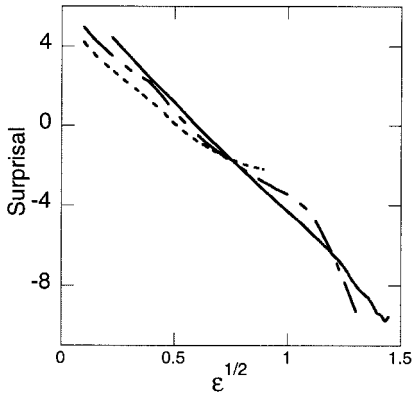

Figure 4. Surprisal plot for the production of cyclic phenyl ions $C_6H_5^+$ as a function of the square root of the translational energy (eqs 4 and 7). (solid line) Production of $C_6D_5^+$ ions (experimental data reported in ref 14). (dotted line) Production of $C_6H_5^+$ ions with experimental data taken from ref 14. (dashed−dotted line) Production of $C_6H_5^+$ ions with data obtained as a private communication from the authors of ref 14 and reported in Figure 1.

For the $C_6H_5^+ + HF$ pair of ions, the constant C is equal to 477 $(cm^{-1})^{-1}$ and $\beta = 0.25$ $(cm^{-1})^{-1/2}$. For the deuterated species one finds $C = 900$ and $\beta = 0.27$, also in the same units.

3. Surprisal Graph for the Major Component

The major broad component of the experimentally determined KERDs (thus relative to production of the cyclic phenyl ion), read in Figures 4 and 5 of ref 14, was obtained by subtracting the minor feature in an arbitrary but reasonable way. The corresponding prior distribution was divided by this result, according to eq 4. Linear surprisal graphs, represented in Figure 4, were obtained when the logarithm of this ratio was plotted as a function of the square root of the translational energy release.

The observed linearity indicates that the particular form of eq 3 valid in the present case is

$$P(\epsilon|E) = P^0(\epsilon|E)\, e^{-\lambda_0}\, e^{-\lambda_1 \epsilon^{1/2}} \tag{7}$$

with $E = 2.50$ or 2.82 eV for the nondeuterated and deuterated ion, respectively. In other words, the constraint that prevents the dynamics from being statistical is the square root of the translational energy, that is, the linear translational momentum of the separating fragments. The identification of the linear momentum as the constraint has been noted in all previous studies.[23−26,40]

The quality of the surprisal graph is excellent for the deuterated species. This is partly due to the weak intensity of the minor component, which makes its subtraction relatively easy. On the other hand, problems linked to the high-energy part of the KERD clearly arise for the nondeuterated species, as shown in Figure 4. This became apparent after an additional KERD relative to the dissociation of $C_6H_5F{\cdot}H^+$, kindly provided by Schröder et al.[14] and represented in Figure 1, was analyzed. The long tail of the KERD is obviously nonphysical. On the other hand, the KERD published as Figure 4 in ref 14 ends up too rapidly.

The Lagrange parameter λ_1 adopts a large and negative value, of the order of -10 $eV^{-1/2}$. This indicates that the translational energy release is substantially larger than the statistical prior estimate obtained by assuming that all quantum states are equally populated. This nonstatistical effect is due to the presence of an energy barrier along the reaction path (Figure 3), a large fraction of which is converted into translational energy. This point will be analyzed in section 5.

4. Entropy Deficiency and Ergodicity Index

The most important concept in a maximum entropy analysis is that of entropy deficiency. With each KERD is associated a dimensionless entropy S. The entropy of the prior (most statistical) distribution, denoted S^{prior}, is necessarily larger than that of the experimental KERD. The difference DS between the entropy of the prior distribution and that of the actual KERD is called the entropy deficiency. It can be demonstrated[16−19] that DS is necessarily a nonnegative quantity:

$$DS = S^{prior} - S = \int_0^E P(\epsilon|E) \ln\left[\frac{P(\epsilon|E)}{P^0(\epsilon|E)}\right] dE = -\lambda_0 - \lambda_1 \langle \epsilon^{1/2} \rangle \geq 0 \tag{8}$$

where

$$\langle \epsilon^{1/2} \rangle = \int_0^E \epsilon^{1/2} P(\epsilon|E) dE \tag{9}$$

A nonzero value for DS implies that the phase space sampled by the pair of fragments is reduced with respect to its maximum value. As a matter of fact, it can be shown that the quantity $\exp(-DS)$ measures the fraction of available phase space effectively sampled by the pair of fragments[33,34] and can therefore be termed an "ergodicity index". In the present case, the Lagrange parameters derived in the previous section lead to values of the ergodicity index $\exp(-DS)$ of the order of 15% for both isotopomers. The situation is not statistical at all because of the presence of the barrier, as analyzed in the next section.

5. Conversion of the Barrier Energy into Translational Energy

The experimental data on the KERDs have been derived from an analysis of metastable (i.e., corresponding to lifetimes of the order of 10^{-5} s) dissociations studied in several field-free regions of a four-sector mass spectrometer.[14] The observed peak shapes are really averages over a distribution of lifetimes and internal energies.[23−25,35] However, it has been analytically demonstrated[28] that average translational energies are fairly insensitive to the collection efficiency of the metastable ions if the entry and exit times in the field-free region are not too different.

When a reverse activation energy barrier occurs along the reaction path, the observed translational energy $\langle \epsilon \rangle$ must be partitioned into two contributions. If E denotes the internal energy and if E_b is the energy of the barrier (both measured with respect to the dissociation asymptote), then, as proposed by Zamir and Levine,[36] one can write

$$\langle \epsilon \rangle = a(E - E_b) + bE_b \tag{10}$$

Equation 10 means that the two components of the energy in excess [i.e., the nonfixed energy of the transition state ($E - E_b$) and the energy of the barrier E_b] are both partly converted into translational energy, but with different efficiencies, measured by the coefficients a and b. Coefficient b can be expected to be larger than coefficient a because the energy of the barrier is preferentially released as translational energy, with a higher efficiency than the internal energy in excess of the barrier ($E - E_b$).

Coefficient a measures the propensity of releasing the nonfixed internal energy as translation in the reaction coordinate. The fact that the constraint that operates on the dynamics is the square root of the kinetic energy (Figure 4) (i.e., the translational momentum of the fragments) indicates the operation of

the so-called momentum gap law, which provides that the nonfixed energy is only reluctantly released as translational energy.[20,23−28,37−39] A bias exists against large translational energy releases, which can be estimated as follows.

Lorquet[28] showed that when the function $N(E)$, representing the density of states of the fragments, can be adequately represented by a simple algebraic expression, the integrations required by the maximum entropy analysis (eqs 1, 8, and 9) can be performed analytically and generate closed-form equations. However, the resulting expressions involve complicated special functions of mathematical physics, most often generalized hypergeometric series. The latter can be generated by a computer program, but it is sometimes possible to approximate them by an empirical equation. When the density of states $N(E)$ varies with the internal energy as expressed in eq 6, the amount of internal energy that is released as translation in the reaction coordinate can be expressed in terms of the rate of increase of the density of states of the pair of fragments (i.e., the quantity β defined in eq 6) and of the fraction of available phase space actually sampled, measured by the quantity $\exp(-DS)$. When the nonfixed energy of the transition state is equal to $(E - E_b)$ (i.e., the energy in excess of the barrier), the coefficient a is given by[28]

$$a = \{0.27/[\beta(E - E_b)^{1/2} + 2.2]\}[1 + 1.85 \exp(-DS)]^2 \quad (11)$$

The numbers that appear in this equation have no special significance. They result from an empirical representation of a combination of generalized hypergeometric functions.

The value of the ergodicity index $\exp(-DS)$ is unknown in the present case. However, from previous experience,[23−28,36,40] it can be estimated conservatively to range between 50% and 95%. This leads to values of a equal to (0.05 ± 0.02) for both isotopomers. Thus, the part of the nonfixed internal energy that is released as translational energy [i.e., the quantity $a\,(E - E_b)$] can be estimated to be about equal to (0.065 ± 0.03) eV and to (0.08 ± 0.03) eV for the normal and deuterated species, respectively.

Coming back to eq 10 and adopting for the average translational energy release values[14] of $\langle\epsilon\rangle = 0.60 \pm 0.05$ or 0.65 ± 0.07 eV, one finally derives values of $b = 0.46 \pm 0.08$ or 0.49 ± 0.08 for the nondeuterated and deuterated cases, respectively.

To summarize, the measured average translational energy of the broad component of the KERD has a double origin. Part of it comes from the translational energy at the top of the barrier. This component represents about 5% of the internal energy in excess of the top of the barrier. The second component results from the (partial) conversion of the energy barrier (about 1.17 eV) into translational energy. The efficiency of this conversion is measured by the coefficient b. The fact that the latter is found to be less than one indicates that the barrier is not entirely converted into translational motion. This results from the operation of exit−channel interactions between separating fragments, that is, indicates that part of the translational energy is converted into rotation (or, less probably, into vibration) of the fragments. Only about one-half of the energy of the barrier is released as translation. Similar orders of magnitude were derived by Aschi and Grandinetti from classical trajectory calculations[41] of the translational energy released in HF loss reactions from small inorganic ions as well as from previous experiments.[42−45]

What causes the exit−channel interactions? Two features of the potential energy surface are relevant in this respect. First, ab initio calculations performed by Hrušák et al.[15] give a good idea of the reaction coordinate. At the top of the barrier, the $C_6H_6F^+$ ion has a nonplanar structure. (In fact, two transition states have been calculated, both nonplanar.) The barrier is followed by a potential well whose minimum corresponds to an ion−neutral complex $C_6H_5^+ \cdot HF$ with a CHF angle equal to about 120°. This sequence of geometries suggests that strong torques operate when the hydrogen fluoride molecule is detached from the phenyl cation. As a result, translation and rotation remain coupled during fragmentation and a substantial part of the kinetic energy is released as rotational motion. Second, the released translational energy can be expected to randomize (at least partly) in the potential well that follows the energy barrier as the nuclear trajectories explore this well, even briefly, during the last step of the dissociation. However, as pointed out by Aschi and Grandinetti,[41] the higher the energy in excess, the lower the efficiency of the randomization process in the potential well of the ion−neutral complex.

6. Production of Open-chain $C_6H_5^+$ Ions

Schröder and co-workers[14] assumed the low-intensity, low-energy component of the KERD derived from the production of open-chain isomer(s) of the phenyl ion. Acyclic isomers have been detected via collision-induced dissociations[46] and in charge-transfer experiments.[47] However, information on their relative energies can only come from ab initio calculations. In what follows, quantum chemical acronyms have their commonly accepted significance.[48,49]

The energy of six different isomers of the $C_6H_5^+$ cation (represented in Figure 5) was calculated with the GAUSSIAN system of programs.[50] To check the stability of the predictions, a sequence of computations was performed with basis sets of increasing size. Adding polarization functions on the hydrogen atoms to the basis set has a very small influence, but transferring from a double- to a triple-dzeta basis set lowers the energy difference between an open-chain isomer and the cyclic structure by about 0.1 eV and sometimes more. The correlation energy was introduced by the presumably reliable quadratic configuration interaction with single and double excitations (QCISD) method.[51] The results, corrected for the zero-point energy, are reported in Table 1. Energies are measured with respect to the cyclic phenyl structure.

The conformation $HC^+{=}CH{-}CH{=}CH{-}C{\equiv}CH$ does not correspond to a stable structure. It spontaneously rearranges into a low-energy, open-chain isomer (hereafter denoted **1**) that is located about 1 eV above to the cyclic phenyl structure. The equilibrium structure is *trans* with respect to the central CC bond; it is about 0.1 eV lower in energy than the *cis* isomer. Isomers $\mathbf{1}_{trans}$ and $\mathbf{1}_{cis}$ cannot be described by a conventional valence notation, for the following reasons. (i) The electronic structure is highly delocalized, as shown by the pattern of CC bond lengths ($R_{12} = 1.29$ Å, $R_{23} = 1.36$ Å, $R_{34} = 1.40$ Å, $R_{45} = 1.40$ Å, $R_{56} = 1.22$ Å). Note especially the near equality of the three internal bonds. (ii) One might invoke a resonance hybrid between at least two structures $H_2C{=}C{=}CH{-}CH^+{-}C{\equiv}CH \leftrightarrow H_2C{=}C^+{-}CH{=}CH{-}C{\equiv}CH \leftrightarrow$ ... On one hand, the CH_2 group is perpendicular to the plane containing the remaining atoms, just as in an allenic structure. The barrier associated with the torsion of the methylene group is as high as 1.2 eV. On the other hand, however, the isomerization barrier between the *cis* and *trans* structures is of the order of 1.3 eV. Such a high value suggests that the two central carbon atoms are connected by a fairly strong bond. (iii) A Mulliken population analysis indicates that more than a positive charge

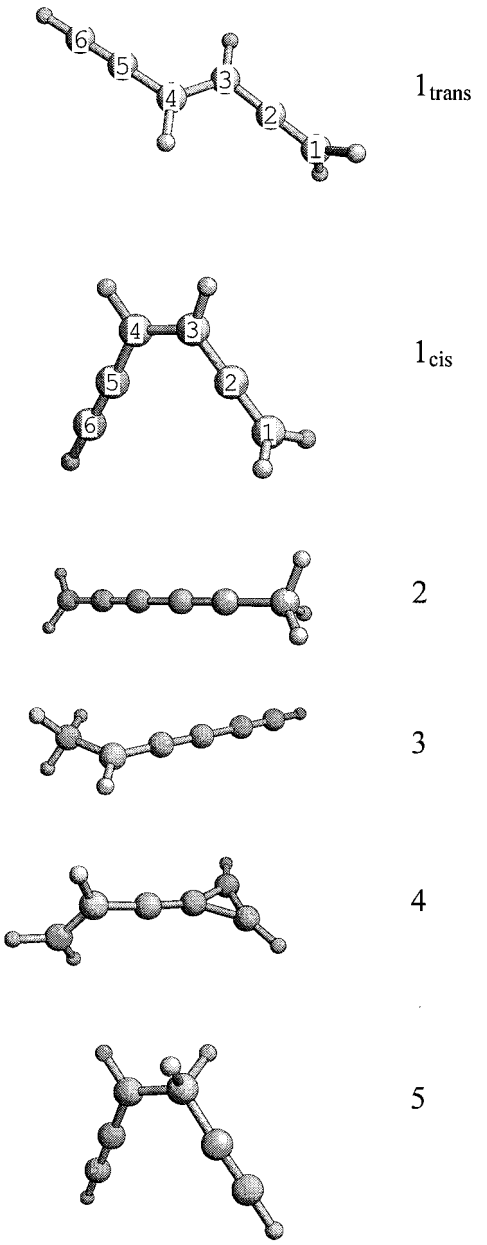

Figure 5. Structure of the open-chain isomers of $C_6H_5^+$ calculated at the QCISD/6-31G(d) level.

is spread over all the atoms including the five hydrogens, with carbons 1, 3, and 6 being strongly *negatively* charged, as usually found in the study of organic cations.[52,53]

Slightly higher in energy comes the quasilinear chain $H_3C-C\equiv C-C\equiv C-CH_2^+$ (denoted **2**), previously identified by Schröder et al.[47] via charge-reversal spectroscopy. Our calculations locate it about 1.2 eV above the cyclic structure.

Another hexadiynyl isomer $HC\equiv C-C\equiv C-CH_2-CH_2^+$ does not correspond to a stable conformation; it spontaneously rearranges to another fairly low-energy structure $HC\equiv C-C\equiv C-CH^+-CH_3$ (**3**), approximately 1.3 eV above the cyclic isomer.

In a similar way, an attempt was made to remove a hydrogen atom from the divinylacetylene isomer (i.e., formally, $H_2C=CH-C\equiv C-CH=CH^+$). However, this structure turned out to be unstable and to cyclize spontaneously to a cyclopropene ring substituted by a three-carbon atom chain (structure **4**), about 1.7 eV above the cyclic structure. Another hexadiynyl isomer, $HC\equiv C-CH_2-CH^+-C\equiv CH$ (**5**), was more than 2 eV above the cyclic conformation.

Because of zero-point energy effects, energy values for the perdeuterated $C_6D_5^+$ isotopomer are higher than those calculated for the $C_6H_5^+$ ion. For isomers **1** and **2**, the magnitude of the energy shift is equal to 0.017 eV.

The vibrational frequencies and rotational constants of the open-chain isomers (and those of the deuterated isotopomers isomers **1** and **2**) were calculated at the B3LYP/6-31G(d) level recommended by Scott and Radom.[31] For the quasiallenic isomer **1**, the lowest torsional frequency calculated at 95 cm^{-1} (86 cm^{-1} for the deuterated isotopomer) was treated as an anharmonic oscillator transforming into a free rotor when its internal energy exceeds 1.0 eV. For the quasilinear isomer **2**, the lowest torsional frequency calculated at 31 cm^{-1} (22 cm^{-1} for the deuterated isotopomer) was replaced by a free internal CH_3 or CD_3 rotor. In the energy range of interest [0.5−1.5] eV, the density of rovibrational states of the two pairs of fragments **1** + HF could again be fitted to eq 6 with $C = 2500$ $(cm^{-1})^{-1}$ and $\beta = 0.28$ $(cm^{-1})^{-1/2}$. (For the deuterated species, in the energy range [0.7−1.8] eV, $C = 19\,000$ and $\beta = 0.29$, also in wavenumber units). Fortunately, the density of states of the pair **2** + HF was not very different. Because it could be parametrized with the same value of the exponent β, a prior distribution common to both open-chain isomers could be calculated from these results.

The experimental KERDs were compared with bimodal distributions obtained by superposing two contributions. (1) A broad and intense component, corresponding to the generation of the cyclic phenyl ion having an internal energy $E = 2.50$ eV (or 2.82 eV for the deuterated species), was calculated from eqs 5−7 with the Lagrange parameters determined in section 3. (2) The minor component was interpreted as resulting from the production of the open-chain isomer $\mathbf{1_{trans}}$ (with a possible admixture of $\mathbf{1_{cis}}$ and of **2**) having an internal energy equal to 2.50−1.00 = 1.50 eV (or 2.82−1.02 = 1.80 eV for the deuterated species). Its Lagrange parameter λ_1 was determined by adjusting the maximum of a distribution given by eq 7 to the most probable energy release experimentally determined by Schröder and co-workers.[14] The parameter λ_1 was found to be positive and of the order of 6 $eV^{-1/2}$ or 5 $eV^{-1/2}$ for the normal and deuterated isotopomers, respectively.

TABLE 1: Ab Initio Calculated Energy Difference (in eV units) between the Open-chain and Cyclic Isomers of the Phenyl Ion, Corrected for the Zero-point Energy

number of basis functions	method	$\mathbf{1}_{trans}$	$\mathbf{1}_{cis}$	**2**	**3**	**4**	**5**
100	B3LYP/6-31G(d)	1.01	1.10	0.96	1.22	1.70	2.34
115	B3LYP/6-31G(d,p)	1.01	1.10	0.98	1.23	1.70	2.34
138	B3LYP/6-311G(d,p)//B3 LYP/6-31G(d,p)	0.87	0.96	0.86	1.10	1.64	2.12
109	B3LYP/cc-pVDZ	1.03	1.13	1.05	1.28	1.77	2.32
183	B3LYP/AUG-cc-pVDZ// B3LYP/cc-pVDZ	1.02	1.12	1.08	1.30	1.76	2.30
250	B3LYP/cc-pVTZ//B3LY P/cc-pVDZ	0.90	0.99	0.89	1.12	1.67	2.15
100	QCISD/6-31G(d)	1.07	1.15	1.31	1.43	1.76	2.16
109	QCISD/cc-pVDZ	1.11	1.19	1.34			2.18
115	QCISD/6-31G(d,p)//QCISD/6-31G(d)	1.08	1.17	1.29	1.42	1.74	2.19
138	QCISD/6-311G(d,p)//QCISD/6-31G(d)	1.00	1.08	1.22	1.32	1.70	2.02

Figures 1 and 2 compare experiment and theory with the relative intensity of the two components taken as a fitting parameter. As was to be expected from Figure 4, the fit is much better for the deuterated compound. The branching ratio between the two channels is estimated to be about 16:1, whereas Schröder et al.[14] proposed 10:1. For the deuterated species, we obtain 34:1, to be compared with the ratio 18:1 derived by Schröder et al. Our numerical values are approximate because the experimental KERDs have been treated as if they had been determined in an energy-resolved experiment. Neglecting the averaging procedure over the collection efficiency in a sector instrument is valid for determination of the first moment of the distribution.[28] However, the accuracy of this approximation is unknown if the fitting is performed on the maximum of the KERD, as has been done for the estimation of the branching ratio between the broad and the minor components.

7. Concluding Remarks

The present calculations confirm the analysis conducted by Schröder et al.[14] concerning the bimodal nature of the KERD. The broad component is due to the production of the cyclic phenyl ion. The major fraction of the observed translational energy release results from the conversion of the energy barrier into translational energy with an efficiency of about 50%. The dynamics is constrained by the momentum gap law, as in all other cases studied so far.

The weaker component corresponds to the formation of one or several open-chain isomers. For simplicity, generation of a single open-chain isomer has been assumed in the present analysis. Competitive production of another low-lying isomer cannot be ruled out by the present method. However, we feel that the sharpness of the weaker component argues against this possibility.

The triplet state of the cyclic phenyl ion is known to lie about 1 eV above its ground state,[54,55] thus in the same energy range as the low-energy, open-chain isomers. However, ab initio calculations by Harvey et al.[56] have shown that the triplet phenyl cation is likely to be a very short-lived species that very rapidly undergoes intersystem crossing to the singlet ground state. Therefore, it is not expected to play a role in reactions taking place on a time scale of the order of 10^{-5} s.

Acknowledgment. We are grateful to Dr. D. Schröder for suggesting the problem, for sending additional data, and critically reading the manuscript. This work has been supported by a research grant from the Actions de Recherche Concertées, Direction de la Recherche Scientifique de la Communauté française de Belgique.

References and Notes

(1) Baer, T.; Hase, W. L. *Unimolecular Reaction Dynamics. Theory and Experiments*; Oxford University Press: New York, 1996.
(2) Baer, T. *Adv. Chem. Phys.* **1986**, *64*, 111.
(3) Lifshitz, C. *Adv. Mass Spectrom.* **1978**, *7A*, 3.
(4) Lifshitz, C. *Int. J. Mass Spectrom. Ion Phys.* **1982**, *43*, 179.
(5) Lifshitz, C. *J. Phys. Chem.* **1983**, *87*, 2304.
(6) Lifshitz, C. *Adv. Mass Spectrom.* **1992**, *12*, 315.
(7) Chesnavich, W. J.; Bowers, M. T. Statistical Methods in Reaction Dynamics. In *Gas-Phase Ion Chemistry*; Bowers, M. T., Ed.; Academic Press: New York, 1979; Vol. 1, p 119.
(8) Derrick, P. J.; Donchi, K. F. Mass spectrometry. In *Chemical Kinetics*; Bamford, C. H., Tipper, C. F. H., Eds.; Elsevier: Amsterdam, 1983; Vol. 24, p 53.
(9) Klots, C. E. *J. Chem. Phys.* **1976**, *64*, 4269.
(10) Powis, I. *Acc. Chem. Res.* **1987**, *20*, 179.
(11) Cho, Y. S.; Choe, J. C.; Kim, M. S. *J. Phys. Chem.* **1995**, *99*, 8645.
(12) Lim, S. H.; Choe, J. C.; Kim, M. S. *J. Phys. Chem. A* **1998**, *102*, 7375.
(13) Moon, J. H.; Choe, J. C.; Kim, M. S. *J. Phys. Chem. A* **2000**, *104*, 458.
(14) Schröder, D.; Oref, I.; Hrušák, J.; Weiske, T.; Nikitin, E. E.; Zummack, W.; Schwarz, H. *J. Phys. Chem. A* **1999**, *103*, 4609.
(15) Hrušák, J.; Schröder, D.; Weiske, T.; Schwarz, H. *J. Am. Chem. Soc.* **1993**, *115*, 2015.
(16) Levine, R. D.; Bernstein, R. B. Thermodynamic Approach to Collision Processes. In *Dynamics of Molecular Collisions, Part B*; Miller, W. H., Ed.; Plenum: New York, 1976; p 323.
(17) Levine, R. D.; Kinsey, J. L. Information-Theoric Approach: Application to Molecular Collisions. In *Atom-Molecule Collision Theory. A Guide for the Experimentalist.*; Bernstein, R. B., Ed.; Plenum: New York, 1979.
(18) Levine, R. D. *Adv. Chem. Phys.* **1981**, *47*, 239.
(19) Levine, R. D. Statistical Dynamics. In *Theory of Chemical Reaction Dynamics*; Baer, M., Ed.; CRC Press: Boca Raton, FL, 1985.
(20) Levine, R. D.; Bernstein, R. B. *Molecular Reaction Dynamics and Chemical Reactivity*; Oxford University: New York, 1987.
(21) Momigny, J.; Locht, R.; Caprace, G. *Int. J. Mass Spectrom. Ion Processes* **1986**, *71*, 159.
(22) Momigny, J.; Locht, R. *Chem. Phys. Lett.* **1993**, *211*, 161.
(23) Urbain, P.; Remacle, F.; Leyh, B.; Lorquet, J. C. *J. Phys. Chem.* **1996**, *100*, 8003.
(24) Urbain, P.; Leyh, B.; Remacle, F.; Lorquet, A. J.; Flammang, R.; Lorquet, J. C. *J. Chem. Phys.* **1999**, *110*, 2911.
(25) Urbain, P.; Leyh, B.; Remacle, F.; Lorquet, J. C. *Int. J. Mass Spectrom.* **1999**, *185/186/187*, 155.
(26) Hoxha, A.; Locht, R.; Lorquet, A. J.; Lorquet, J. C.; Leyh, B. *J. Chem. Phys.* **1999**, *111*, 9259.
(27) Lorquet, J. C. *Int. J. Mass Spectrom.* **2000**, *201*, 59.
(28) Lorquet, J. C. *J. Phys. Chem. A* **2000**, *104*, 5422.
(29) Illenberger, E.; Momigny, J. *Gaseous Molecular Ions*; Springer-Verlag: New York, 1992.
(30) Gilbert, R. G.; Smith, S. C. *Theory of Unimolecular and Recombination Reactions*; Blackwell Scientific Publications: Oxford, UK, 1990.
(31) Scott, A. P.; Radom, L. *J. Phys. Chem.* **1996**, *100*, 16502.
(32) Klippenstein, S. J. *Int. J. Mass Spectrom. Ion Processes* **1997**, *167/168*, 235.
(33) Iachello, F.; Levine, R. D. *Europhys. Lett.* **1987**, *4*, 389.
(34) Levine, R. D. *Adv. Chem. Phys.* **1988**, *70*, 53.
(35) Holmes, J. L.; Terlouw, J. K. *Org. Mass Spectrom.* **1980**, *15*, 383.
(36) Zamir, E.; Levine, R. D. *Chem. Phys.* **1980**, *52*, 253.
(37) Beswick, J. A.; Jortner, J. *Adv. Chem. Phys.* **1981**, *47*, 363.
(38) Ewing, G. E. *J. Chem. Phys.* **1979**, *71*, 3143.
(39) Ewing, G. E. *J. Chem. Phys.* **1980**, *72*, 2096.
(40) Hoxha, A.; Locht, R.; Lorquet, J. C.; Leyh, B. **2001**, manuscript submitted for publication.
(41) Aschi, M.; Grandinetti, F. *Eur. J. Mass Spectrom.* **2000**, *6*, 31.
(42) Aschi, M.; Grandinetti, F.; Pepi, F. *Int. J. Mass Spectrom. Ion Proc.* **1994**, *130*, 117.
(43) Aschi, M.; Cacace, F.; Grandinetti, F.; Pepi, F. *J. Phys. Chem.* **1994**, *98*, 2713.
(44) Cacace, F.; Grandinetti, F.; Pepi, F. *Inorg. Chem.* **1995**, *34*, 1325.
(45) Grandinetti, F.; Hrušák, J.; Schröder, D.; Karass, S.; Schwarz, H. *J. Am. Chem. Soc.* **1992**, *114*, 2806.
(46) Eyler, J. R.; Campana, J. E. *Int. J. Mass Spectrom. Ion Processes* **1983**, *55*, 171.
(47) Schröder, D.; Schroeter, K.; Zummack, W.; Schwarz, H. *J. Am. Soc. Mass Spectrom.* **1999**, *10*, 878.
(48) Hehre, W. J.; Radom, L.; Schleyer, P. v. R.; Pople, J. A. *Ab Initio Molecular Orbital Theory*; Wiley: New York, 1986.
(49) Jensen, F. *Introduction to Computational Chemistry*; Wiley: Chichester, 1999.
(50) Frisch, M. J.; Trucks, G. W.; Schlegel, H. B.; Gill, P. M. W.; Johnson, B. G.; Robb, M. A.; Cheeseman, J. R.; Keith, T.; Petersson, G. A.; Montgomery, J. A.; Raghavachari, K.; Al-Laham, M. A.; Zakrzewski, V. G.; Ortiz, J. V.; Foresman, J. B.; Peng, C. Y.; Ayala, P. Y.; Chen, W.; Wong, M. W.; Andres, J. L.; Replogle, E. S.; Gomperts, R.; Martin, R. L.; Fox, D. J.; Binkley, J. S.; Defrees, D. J.; Baker, J.; Stewart, J. P.; Head-Gordon, M.; Gonzalez, C.; Pople, J. A. *Gaussian 94*, Revision B.3; Gaussian, Inc.: Pittsburgh, PA, 1995.
(51) Chuang, Y. Y.; Coitino, E. L.; Truhlar, D. G. *J. Phys. Chem. A* **2000**, *104*, 446.
(52) Lorquet, J. C. *Int. J. Mass Spectrom.* **2000**, *200*, 000.
(53) Wiberg, K. B.; Schleyer, P. von Rague; Streitwieser, A. *Can. J. Chem.* **1996**, *74*, 892.
(54) Hrušák, J.; Schröder, D.; Iwata, S. *J. Chem. Phys.* **1997**, *106*, 7541.
(55) Nicolaides, A.; Smith, D. M.; Jensen, F.; Radom, L. *J. Am. Chem. Soc.* **1997**, *119*, 8083.
(56) Harvey, J. N.; Aschi, M.; Schwarz, H.; Koch, W. *Theor. Chem. Acc.* **1998**, *99*, 95.